ACS Catalysis

Letter

Cite This: ACS Catal. 2019, 9, 474−478

pubs.acs.org/acscatalysis

Operando Spectroscopic Investigations of Copper and Oxide-Derived Copper Catalysts for Electrochemical CO Reduction

Arnav S. Malkani, Marco Dunwell, and Bingjun Xu*

Center for Catalytic Science and Technology, Department of Chemical and Biomolecular Engineering, University of Delaware, Newark, Delaware 19716, United States

Supporting Information

ABSTRACT: Oxide-derived copper (OD-Cu) has been shown to favor C_2 and C_3 products in electrochemical CO reduction at lower overpotentials than polycrystalline copper (Cu-poly). Despite numerous studies and proposed mechanisms, the exact nature of the active phase is still a topic of discussion. In this work, we employ operando attenuated total reflection surface enhanced infrared absorption spectroscopy (ATR-SEIRAS) to investigate different sites available on Cu-poly and OD-Cu surfaces using CO as a probe molecule. We identify a CO adsorption band on OD-Cu at 2058 cm^{-1} that is different from those on Cu-poly but resembles CO bound to the Cu(100) facet. In accordance with reactivity studies, we propose that this band corresponding to distinct CO binding sites is responsible for OD-Cu's enhanced CO reduction activity.

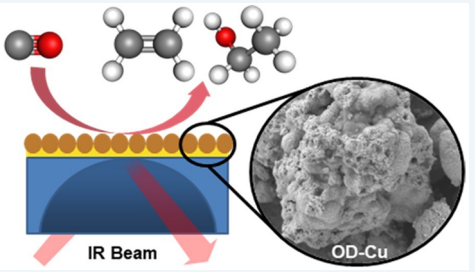

KEYWORDS: *ATR-SEIRAS, C−C coupling, CO reduction, copper, electrochemistry, operando study, oxide-derived copper*

CO_2 and CO reduction reactions (CO_2RR and CORR, respectively) powered by renewable electricity are key electrochemical transformations in mitigating anthropogenic climate change.[1] The ability to produce high-value chemicals and fuels through these reactions is crucial to their large-scale implementation. CORR has received recent attention because CO is a known intermediate in the formation of C_{2+} hydrocarbons and oxygenates in CO_2RR.[2,3] Copper is the only metal with appreciable selectivity for hydrocarbons and oxygenates in CO_2RR and CORR, however, only at high overpotentials.[4]

Among the strategies to improve the selectivity for C_{2+} products in CORR, OD-Cu developed by the Kanan group stood out. OD-Cu was shown to favor C−C coupling reactions at low overpotentials (e.g., a Faradaic efficiency (FE) toward C_2 products of 57% at −0.3 V).[5] All voltages in this work are referenced to the reversible hydrogen electrode (RHE) unless otherwise noted. The enhanced activity and selectivity for C−C coupling on OD-Cu were attributed to the presence of strong CO binding sites on grain boundaries;[5,6] however, the exact nature and structure of these active sites remain unclear. Alternatively, increased roughness of Cu surfaces has been proposed to be in part responsible for the enhanced selectivity for C−C coupling reactions on roughened and nanostructured Cu catalysts.[7−9] Earlier work by Hori et al. showed that rougher electrodes promote the formation of C_2 products like ethane.[2] The Kenis group found that higher current densities toward C_2 products were obtained in an electrolyzer when using Cu nanoparticles with the highest surface roughness.[10] Jeon et al. showed similar trends with rough Cu prism nanocatalysts and suggested that surface roughness was the cause for the enhanced C−C coupling.[11] In addition, trace amounts of residual oxygen from the CuO used to form OD-Cu have been proposed to generate active sites responsible for its enhanced activity. Mistry et al. proposed that the Cu^+ sites formed from residual oxygen are the active sites for the CORR; however, the residual oxygen disappeared after an hour of reduction.[12] Eilert et al. claimed that subsurface oxygen detected by X-ray photoelectron spectroscopy and transmission electron microscopy electron energy loss spectroscopy may aid in the stabilization of CO to the surface.[13] However, isotopic labeling studies by Lum et al. using secondary ion mass spectrometry showed that the top 100 nm of the Cu surface did not have oxygen during CO_2RR conditions.[14] Similarly, in situ Raman spectroscopy conducted by Yeo and co-workers showed that Cu_2O vibrations disappeared within 200 s at −0.99 V.[15,16]

The discussion in recent literature regarding the origin of enhanced C−C coupling activity on OD-Cu and nanostructured Cu for CORR could be at least in part attributed to the difficulty in establishing a reliable correlation between the activity and active sites present during reaction. In particular, the scarcity of operando characterization techniques is a key barrier. We recently developed an operando cell for ATR-SEIRAS (Figure 1) which enables characterization of catalysts under identical conditions to CORR. In this work, we employ operando ATR-SEIRAS to identify distinct CO binding sites on OD-Cu compared with Cu-poly that are responsible for the C−C coupling reaction in CORR at a low

Received: October 23, 2018
Revised: November 27, 2018
Published: December 13, 2018

DOI: 10.1021/acscatal.8b04269
ACS Catal. 2019, 9, 474−478

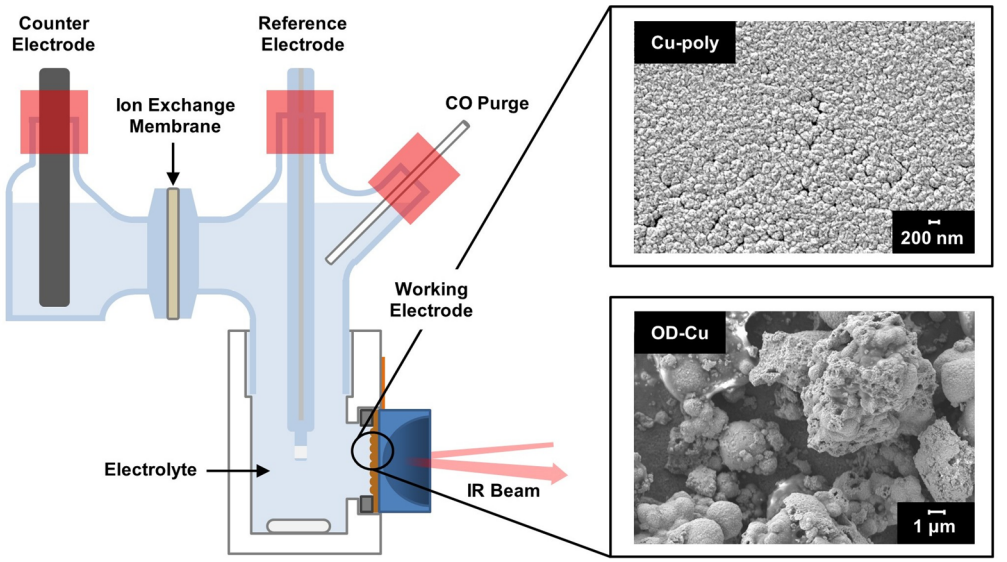

Figure 1. Stirred spectroscopic cell used for all measurements in CO saturated 0.05 M KOH with Cu-poly or OD-Cu particles as a working electrode, graphite rod counter electrode, and an Ag/AgCl reference electrode. Inset: Scanning electron microscope images of Cu-poly and OD-Cu on a gold film.

overpotential (−0.4 V) and correlate these findings with reactivity studies.

The product distribution in CORR on OD-Cu and Cu-poly surfaces at −0.4 V in a reactivity cell (Figure S1) under otherwise identical conditions shows that OD-Cu is uniquely effective in catalyzing C−C coupling reactions at low overpotentials. C_2 and C_3 hydrocarbons and oxygenates are produced with a combined Faradaic efficiency of over 20% on OD-Cu, whereas only hydrogen is detected on Cu-poly (Figure 2). These results are consistent with the literature.[4,5,17] The relatively poor charge balances for the OD-Cu samples are likely due to the reduction of poorly connected CuO particles during reaction. Cyclic voltammograms of OD-Cu and Cu-poly do not reveal any detectable differences that could account for the drastic difference in product distribution (Figure S2).

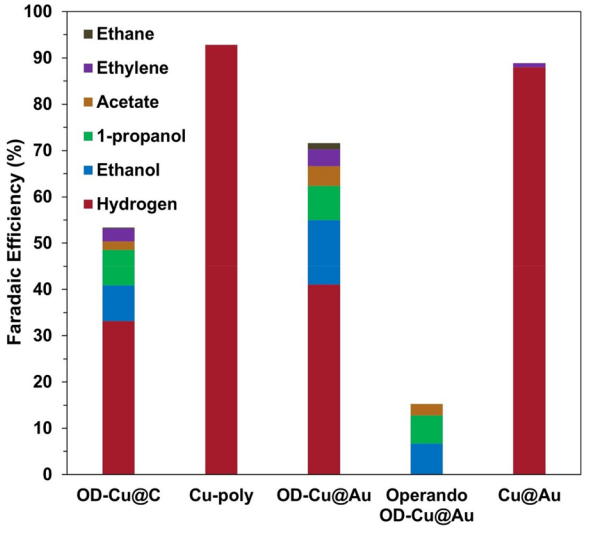

Figure 2. Faradaic efficiency of products formed in CORR on OD-Cu@C, Cu-poly, OD-Cu@Au, operando OD-Cu@Au and Cu@Au in CO saturated KOH at −0.4 V vs RHE.

Operando ATR-SEIRAS studies reveal that there are multiple distinct CO_{ad} sites on the Cu-poly surface. When the Cu-poly surface is first brought to −0.4 V in CO-saturated 0.05 M KOH, one band centered at 2073 cm^{-1} and a weak shoulder at 2089 cm^{-1} are observed (Figure 3, bottom trace). Adsorbed CO bands located in the 2000−2150 cm^{-1} region are generally attributed to linearly bound CO.[3,18,19] In

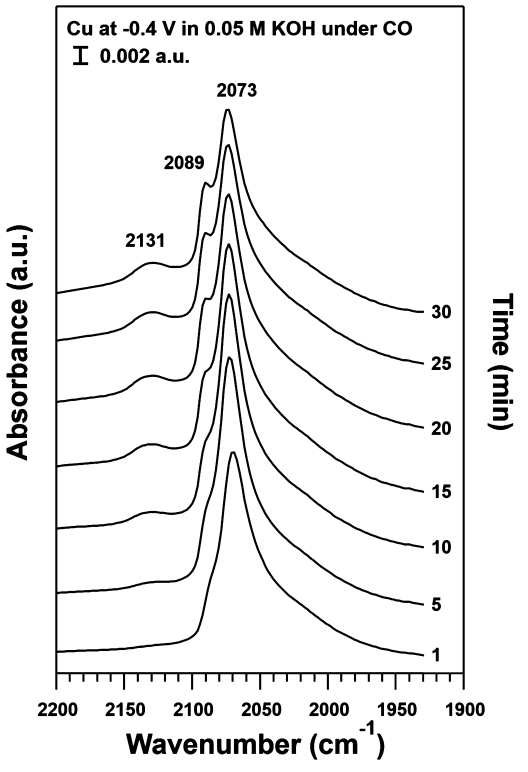

Figure 3. Operando ATR-SEIRAS spectra at −0.4 V vs RHE in CO saturated 0.05 M KOH showing the time evolution of the different CO binding sites on Cu-poly. Spectra presented correspond to 64 coadded scans collected with a 4 cm^{-1} resolution.

DOI: 10.1021/acscatal.8b04269
ACS Catal. 2019, 9, 474−478

particular, the two CO_{ad} bands that are 15 cm^{-1} apart on Cu surfaces have been assigned to CO bound to step (higher wavenumber) and terrace (lower wavenumber) sites.[20−22] The intensity of the 2089 cm^{-1} peak increases at the expense of the 2073 cm^{-1} peak with time as the potential is held at −0.4 V for 30 min (Figure 3). We note that the system is saturated with CO before applying the potential, so the change in relative intensity of the two bands with time cannot be explained by CO slowly populating the surface. The peak intensity of adsorbed CO typically equilibrates to a constant intensity within 1 min in a CO atmosphere. The intensity of the 2089 cm^{-1} peak is enhanced via dipole−dipole coupling with the 2073 cm^{-1} band so the intensities of these two bands are not representative of the actual populations of the two types of surface sites.[21] Previous ATR-SEIRAS studies on CO adsorption on Cu showed only a single band centered around 2075 cm^{-1}.[3,23] The difference between our results and these studies could be attributed to the fact that those experiments were conducted in less alkaline electrolytes (bicarbonate, Figure S3).

The evolving spectra with time suggest that the Cu-poly surface undergoes reconstruction at −0.4 V in the presence of CO, which is consistent with recent reports.[23,24] Interestingly, a band at 2131 cm^{-1} appears over the course of 30 min, which has been assigned to CO adsorbed on Cu^{+}.[25,26] It is unlikely that metallic Cu is oxidized to Cu_2O at a potential (−0.4 V) much lower than the equilibrium potential for its oxide phases (~0.5 V),[27] so we attribute this feature to CO_{ad}, either on reconstructed Cu sites[24] or interacting with cationic species in the electrical double layer (e.g., K^{+}). Further investigations are needed to elucidate the origin of this band. We do not observe any spectroscopic feature attributable to CO adsorbed on CuO_x, which has been suggested to promote the reduction of CO and CO_2. To ensure the 2131 cm^{-1} band is not caused by contaminants in the electrolyte electrochemically deposited on the electrode surface at −0.4 V, control experiments are conducted with a gold film, as well as in $KHCO_3$ produced by CO_2 saturating KOH on the Cu-poly surface, under otherwise identical conditions. No CO adsorption band at ~2130 cm^{-1} is observed in either case (Figure S4 and S5), confirming that this band corresponds to CO adsorbed on Cu sites.

Operando ATR-SEIRAS investigations on OD-Cu particles suggest that they possess distinct CO binding sites aside from those present on the Cu-poly surface. CuO particles are sprayed on to a polycrystalline Cu film and then electrochemically reduced to OD-Cu (OD-Cu@Cu). The loading of CuO particles is between 0.6 and 0.8 mg/cm^2, comparable to those in the reactivity tests. When OD-Cu@Cu is brought to −0.4 V in CO saturated 0.05 M KOH, the spectrum looks similar to that of Cu-poly (Figure 4a,b), which suggests that either they possess similar sites or the signal from OD-Cu in the OD-Cu@Cu sample is overwhelmed by that of the Cu substrate. To differentiate these two possibilities, we conduct a similar experiment using OD-Cu particles supported on a gold film (OD-Cu@Au). Au is employed as the substrate as it does not adsorb CO at the relevant potentials (<−0.1 V, Figure S4). The intensity of CO bands on OD-Cu@Au is almost 2 orders of magnitude lower than that on Cu-poly. This difference could be attributed to the micron-size of the OD-Cu particles and the fact that the evanescent wave in SEIRAS only probes 5−10 nm from the SEIRA-active Au film[28] so only a small fraction of the OD-Cu particles is sampled. Importantly, in addition to bands similar to those on Cu-poly (2073, 2089, and 2131 cm^{-1}), a prominent band at 2058 cm^{-1} is observed (Figures 4c and S6), demonstrating that OD-Cu possesses distinct sites from those on Cu-poly surfaces. To exclude the possibility that the 2058 cm^{-1} band is caused by CO adsorbed on sites at the Cu/Au interface, a control experiment with micron-size Cu particles supported on a gold film (Cu@Au) is also conducted. Only CO adsorption bands similar to those on Cu-poly appear (Figure 4d) with almost no C−C coupling products (Figure 2). This confirms that the 2058 cm^{-1} band corresponds to CO adsorbed on OD-Cu sites. All spectra in Figure 4 are taken at −0.4 V when spectra no longer change with time (i.e., at the steady state). SEM images of fresh and spent catalysts (Figure S7) reveal no discernible morphological changes. Faradaic efficiencies of liquid phase products in CORR on OD-Cu@Au in the spectroscopic cell are similar to those on OD-Cu in the reactivity study (Figures 2 and S8), demonstrating that the spectroscopic tests are conducted under operando conditions. Gaseous products are not quantified in the spectroscopic experiments because CO is continuously bubbled throughout the test.

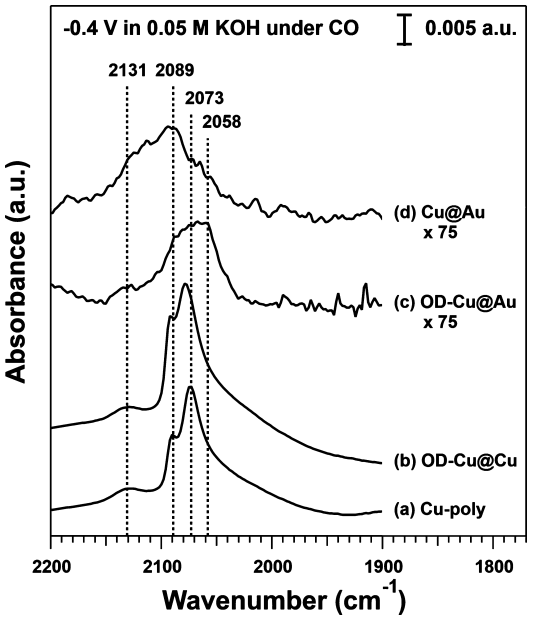

Figure 4. Operando ATR-SEIRAS spectra showing CO binding sites on different catalyst surfaces at −0.4 V vs RHE in CO saturated 0.05 M KOH. Spectra presented correspond to 64 coadded scans collected with a 4 cm^{-1} resolution.

The combined reactivity and operando spectroscopic investigations indicate that the CO adsorption sites corresponding to the band at 2058 cm^{-1} are most likely correlated with OD-Cu's ability to facilitate C−C coupling reactions at low overpotentials. CO adsorption sites corresponding to the 2073, 2089, and 2131 cm^{-1} bands are shared by both Cu-poly and OD-Cu (despite slight differences in their relative intensities among the surfaces investigated in this work), and thus, they cannot account for the difference in the product distribution on these two materials. The 2058 cm^{-1} band is similar to the CO adsorption band observed on the Cu(100) surface at a similar potential vs the standard hydrogen electrode potential by Hori et al.[29] Thus, we hypothesize that OD-Cu preferentially exposes the (100) facet which enhances its CORR activity at low overpotentials. This is consistent with a number of recent experimental and

DOI: 10.1021/acscatal.8b04269
ACS Catal. 2019, 9, 474−478

computational studies claiming that Cu(100) is particularly effective in mediating C−C coupling. Schouten et al. experimentally showed that ethylene formation begins at a lower overpotential on Cu(100) than Cu(111).[30] Jiang et al. attributed the superior C−C coupling activity primarily to the (100) facet of Cu which showed the lowest activation barrier for the C−C coupling step.[31] This peak assignment is consistent with the lower wavenumber of the distinct band on OD-Cu compared to those present on Cu-poly because of the stronger interaction of CO with undercoordinated (100) sites.[32] The presence of strong CO binding sites on OD-Cu also agrees with the recent temperature-programmed desorption report of CO from Cu surfaces.[6] However, we do not observe the CO dimer species reported by Koper and coworkers, possibly due to the interference of bending mode of water and absorbance of Si.[33]

In summary, we demonstrate that OD-Cu possesses distinct CO adsorption sites from those on Cu-poly via operando ATR-SEIRAS, and correlate the presence of these sites with OD-Cu's ability to facilitate C−C coupling in CORR at −0.4 V. The distinct CO adsorption band at 2058 cm^{-1} on OD-Cu could be attributed to the preferentially exposed Cu(100) facet.

■ ASSOCIATED CONTENT

Supporting Information

The Supporting Information is available free of charge on the ACS Publications website at DOI: 10.1021/acscatal.8b04269.

Additional content includes detailed experimental methods, reactivity cell sketch, cyclic voltammograms, supplementary ATR-SEIRAS spectra, NMR spectra, and SEM images of working electrodes (PDF)

■ AUTHOR INFORMATION

Corresponding Author

*E-mail: bxu@udel.edu.

ORCID

Bingjun Xu: 0000-0002-2303-257X

Notes

The authors declare no competing financial interest.

■ ACKNOWLEDGMENTS

This work is supported by the National Science Foundation CAREER Program (Award No. CBET-1651625). The authors thank the Keck Center for Advanced Microscopy and Microanalysis for help with SEM imaging as well as the University of Delaware College of Engineering Machine Shop for the fabrication of custom spectro-electrochemical cells. The authors also thank Mathew Jouny for help with OD-Cu particle preparation.

■ REFERENCES

(1) Pander, J. E.; Ren, D.; Huang, Y.; Loo, N. W. X.; Hong, S. H. L.; Yeo, B. S. Understanding the Heterogeneous Electrocatalytic Reduction of Carbon Dioxide on Oxide-Derived Catalysts. *ChemElectroChem* **2018**, *5*, 219−237.

(2) Hori, Y.; Takahashi, R.; Yoshinami, Y.; Murata, A. Electrochemical Reduction of CO at a Copper Electrode. *J. Phys. Chem. B* **1997**, *101*, 7075−7081.

(3) Wuttig, A.; Liu, C.; Peng, Q.; Yaguchi, M.; Hendon, C. H.; Motobayashi, K.; Ye, S.; Osawa, M.; Surendranath, Y. Tracking a Common Surface-Bound Intermediate during CO_2-to-Fuels Catalysis. *ACS Cent. Sci.* **2016**, *2*, 522−528.

(4) Hori, Y. In *Modern Aspects of Electrochemistry*; Vayenas, C. G., White, R. E., Gamboa-Aldeco, M. E., Eds.; Springer: New York, 2008; Vol. *42*, pp 89−189.

(5) Li, C. W.; Ciston, J.; Kanan, M. W. Electroreduction of Carbon Monoxide to Liquid Fuel on Oxide-Derived Nanocrystalline Copper. *Nature* **2014**, *508*, 504−507.

(6) Verdaguer-Casadevall, A.; Li, C. W.; Johansson, T. P.; Scott, S. B.; McKeown, J. T.; Kumar, M.; Stephens, I. E. L.; Kanan, M. W.; Chorkendorff, I. Probing the Active Surface Sites for CO Reduction on Oxide-Derived Copper Electrocatalysts. *J. Am. Chem. Soc.* **2015**, *137*, 9808−9811.

(7) Li, C. W.; Kanan, M. W. CO_2 Reduction at Low Overpotential on Cu Electrodes Resulting from the Reduction of Thick Cu_2O Films. *J. Am. Chem. Soc.* **2012**, *134*, 7231−7234.

(8) Handoko, A. D.; Ong, C. W.; Huang, Y.; Lee, Z. G.; Lin, L.; Panetti, G. B.; Yeo, B. S. Mechanistic Insights into the Selective Electroreduction of Carbon Dioxide to Ethylene on Cu_2O-Derived Copper Catalysts. *J. Phys. Chem. C* **2016**, *120*, 20058−20067.

(9) Bertheussen, E.; Hogg, T. V.; Abghoui, Y.; Engstfeld, A. K.; Chorkendorff, I.; Stephens, I. E. L. Electroreduction of CO on Polycrystalline Copper at Low Overpotentials. *ACS Energy Lett.* **2018**, *3*, 634−640.

(10) Ma, S.; Sadakiyo, M.; Luo, R.; Heima, M.; Yamauchi, M.; Kenis, P. J. A. One-Step Electrosynthesis of Ethylene and Ethanol from CO_2 in an Alkaline Electrolyzer. *J. Power Sources* **2016**, *301*, 219−228.

(11) Jeon, H. S.; Kunze, S.; Scholten, F.; Roldan Cuenya, B. Prism-Shaped Cu Nanocatalysts for Electrochemical CO_2 Reduction to Ethylene. *ACS Catal.* **2018**, *8*, 531−535.

(12) Mistry, H.; Varela, A. S.; Bonifacio, C. S.; Zegkinoglou, I.; Sinev, I.; Choi, Y.-W.; Kisslinger, K.; Stach, E. A.; Yang, J. C.; Strasser, P.; Roldan Cuenya, B. Highly Selective Plasma-Activated Copper Catalysts for Carbon Dioxide Reduction to Ethylene. *Nat. Commun.* **2016**, *7*, 12123.

(13) Eilert, A.; Cavalca, F.; Roberts, F. S.; Osterwalder, J.; Liu, C.; Favaro, M.; Crumlin, E. J.; Ogasawara, H.; Friebel, D.; Pettersson, L. G. M.; Nilsson, A. Subsurface Oxygen in Oxide-Derived Copper Electrocatalysts for Carbon Dioxide Reduction. *J. Phys. Chem. Lett.* **2017**, *8*, 285−290.

(14) Lum, Y.; Ager, J. W. Stability of Residual Oxides in Oxide-Derived Copper Catalysts for Electrochemical CO_2 Reduction Investigated With ^{18}O Labeling. *Angew. Chem., Int. Ed.* **2018**, *57*, 551−554.

(15) Ren, D.; Deng, Y.; Handoko, A. D.; Chen, C. S.; Malkhandi, S.; Yeo, B. S. Selective Electrochemical Reduction of Carbon Dioxide to Ethylene and Ethanol on Copper(I) Oxide Catalysts. *ACS Catal.* **2015**, *5*, 2814−2821.

(16) Mandal, L.; Yang, K. R.; Motapothula, M. R.; Ren, D.; Lobaccaro, P.; Patra, A.; Sherburne, M.; Batista, V. S.; Yeo, B. S.; Ager, J. W.; Martin, J.; Venkatesan, T. Investigating the Role of Copper Oxide in Electrochemical CO_2 Reduction in Real Time. *ACS Appl. Mater. Interfaces* **2018**, *10*, 8574−8584.

(17) Roberts, F. S.; Kuhl, K. P.; Nilsson, A. Electroreduction of Carbon Monoxide over a Copper Nanocube Catalyst: Surface Structure and pH Dependence on Selectivity. *ChemCatChem* **2016**, *8*, 1119−1124.

(18) Salimon, J.; Hernández-Romero, R. M.; Kalaji, M. The Dynamics of the Conversion of Linear to Bridge Bonded CO on Cu. *J. Electroanal. Chem.* **2002**, *538*−*539*, 99−108.

(19) Hollins, P.; Pritchard, J. Infrared Studies of Chemisorbed Layers on Single Crystals. *Prog. Surf. Sci.* **1985**, *19*, 275−349.

(20) Hollins, P.; Davies, K. J.; Pritchard, J. Infrared Spectra of CO Chemisorbed on a Surface Vicinal to Cu(110): The Influence of Defect Sites. *Surf. Sci.* **1984**, *138*, 75−83.

(21) Hollins, P. The Influence of Surface Defects on the Infrared Spectra of Adsorbed Species. *Surf. Sci. Rep.* **1992**, *16*, 51−94.

DOI: 10.1021/acscatal.8b04269
ACS Catal. 2019, 9, 474−478

(22) Borguet, E.; Dai, H. L. Site-Specific Properties and Dynamical Dipole Coupling of CO Molecules Adsorbed on a Vicinal Cu(100) Surface. *J. Chem. Phys.* **1994**, *101*, 9080−9095.
(23) Gunathunge, C. M.; Li, X.; Li, J.; Hicks, R. P.; Ovalle, V. J.; Waegele, M. M. Spectroscopic Observation of Reversible Surface Reconstruction of Copper Electrodes under CO_2 Reduction. *J. Phys. Chem. C* **2017**, *121*, 12337−12344.
(24) Kim, Y. G.; Baricuatro, J. H.; Javier, A.; Gregoire, J. M.; Soriaga, M. P. The Evolution of the Polycrystalline Copper Surface, First to Cu(111) and Then to Cu(100), at a Fixed CO_2RR Potential: A Study by Operando EC-STM. *Langmuir* **2014**, *30*, 15053−15056.
(25) Scarano, D.; Bordiga, S.; Lamberti, C.; Spoto, G.; Ricchiardi, G.; Zecchina, A.; Otero Areán, C. FTIR Study of the Interaction of CO with Pure and Silica-Supported Copper (I) Oxide. *Surf. Sci.* **1998**, *411*, 272−285.
(26) Bordiga, S.; Pazé, C.; Berlier, G.; Scarano, D.; Spoto, G.; Zecchina, A.; Lamberti, C. Interaction of N_2, CO and NO with Cu-Exchanged ETS-10: A Compared FTIR Study with Other Cu-Zeolites and with Dispersed Cu_2O. *Catal. Today* **2001**, *70*, 91−105.
(27) Protopopoff, E.; Marcus, P. Potential-pH Diagrams for Hydroxyl and Hydrogen Adsorbed on a Copper Surface. *Electrochim. Acta* **2005**, *51*, 408−417.
(28) Osawa, M. Surface-Enhanced Infrared Absorption. *Top. Appl. Phys.* **2001**, *81*, 163−187.
(29) Hori, Y.; Koga, O.; Watanabe, Y.; Matsuo, T. FTIR Measurements of Charge Displacement Adsorption of CO on Poly- and Single Crystal (100) of Cu Electrodes. *Electrochim. Acta* **1998**, *44*, 1389−1395.
(30) Schouten, K. J. P.; Pérez Gallent, E.; Koper, M. T. M. The Influence of pH on the Reduction of CO and CO_2 to Hydrocarbons on Copper Electrodes. *J. Electroanal. Chem.* **2014**, *716*, 53−57.
(31) Jiang, K.; Sandberg, R. B.; Akey, A. J.; Liu, X.; Bell, D. C.; Nørskov, J. K.; Chan, K.; Wang, H. Metal Ion Cycling of Cu Foil for Selective C−C Coupling in Electrochemical CO_2 Reduction. *Nat. Catal.* **2018**, *1*, 111−119.
(32) Bistoni, G.; Rampino, S.; Scafuri, N.; Ciancaleoni, G.; Zuccaccia, D.; Belpassi, L.; Tarantelli, F. How π Back-Donation Quantitatively Controls the CO Stretching Response in Classical and Non-Classical Metal Carbonyl Complexes. *Chem. Sci.* **2016**, *7*, 1174−1184.
(33) Pérez-Gallent, E.; Figueiredo, M. C.; Calle-Vallejo, F.; Koper, M. T. M. Spectroscopic Observation of a Hydrogenated CO Dimer Intermediate During CO Reduction on Cu(100) Electrodes. *Angew. Chem., Int. Ed.* **2017**, *56*, 3621−3624.

DOI: 10.1021/acscatal.8b04269
ACS Catal. 2019, 9, 474−478